NLRP3 inflammasome blockade reduces liver inflammation and fibrosis in experimental NASH in mice

Auvro R. Mridha, Alexander Wree, Avril A.B. Robertson, Matthew M. Yeh, Casey D. Johnson, Derrick M. Van Rooyen, Fahrettin Haczeyni, Narci C.-H. Teoh, Christopher Savard, George N. Ioannou, Seth L. Masters, Kate Schroder, Matthew A. Cooper, Ariel E. Feldstein, Geoffrey C. Farrell

Table of content

Supplementary Table 1. Sequences of primers used for quantitative PCR.

mRNA	Primer Sequences	
Asc	FWD	5'-CTT GTC AGG GGATGA ACT CAA AA-3
	REV	5'-GCC ATA CGA CTC CAG ATA GTA GC-3'
Col1a1	FWD	5'-GCT CCT CTT AGG GGC CAC T-3'
	REV	5'-CCA CGT CTC ACC ATT GGG G-3'
Ctgf	FWD	5'-GGG CCT CTT CTG CGA TTT C-3'
	REV	5'-ATC CAG GCA AGT GCA TTG GTA-3'
F4/80	FWD	5'-TGA CTC ACC TTG TGG TCC TAA-3'
	REV	5'- CTT CCC AGA ATC CAG TCT TTC C-3'
Ly6c	FWD	5'-GCA GTG CTA CGA GTG CTA TGG-3'
	REV	5'-ACT GAC GGG TCT TTA GTT TCC TT-3'
Mpo	FWD	5'-AGT TGT GCT GAG CTG TAT GGA-3'
	REV	5'-CGG CTG CTT GAA GTA AAA CAG G-3'
Casp1	FWD	5'-ACA AGG CAC GGG ACC TAT G-3'
	REV	5'-TCC CAG TCA GTC CTG GAA ATG-3'
Il1b	FWD	5'-GAA ATG CCA CCT TTT GAC AGT G-3'
	REV	5'-CTG GAT GCT CTC ATC AGG ACA-3'
Timp1	FWD	5'-CTT GGT TCC CTG GCG TAC TC-3'
	REV	5'-ACC TGA TCC GTC CAC AAA CAG-3'

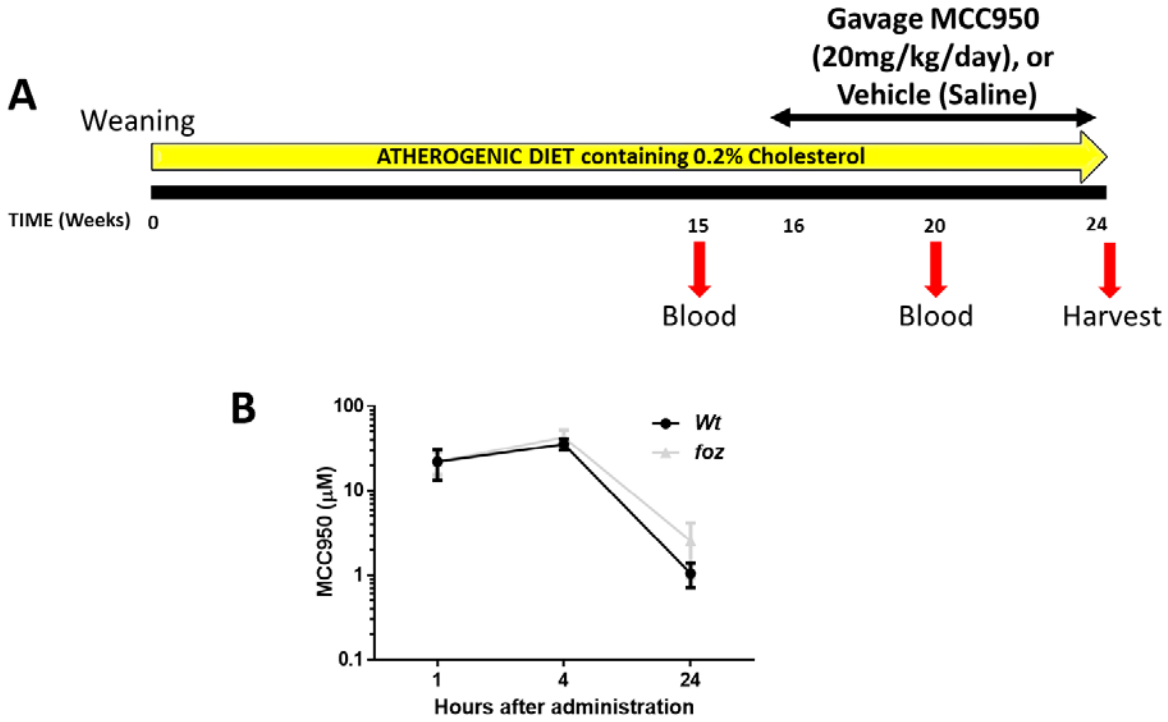

Supplementary Figure 1. (A) Experimental protocol for *in vivo* experiments in wildtype (*Wt*) or *foz/foz* mice fed atherogenic diet, and gavaged with MCC950 or vehicle (saline) from week 16. Blood (~0.20 mL) was collected at 15 and 20 weeks by cheek vein puncture in unanesthetized mice, or cardiac puncture under anesthesia at week 24. (B) Plasma concentration of MCC950 at indicated times after gavage of *foz/foz* or wildtype (*Wt*) mice with MCC950 (20 mg/kg body weight).

.

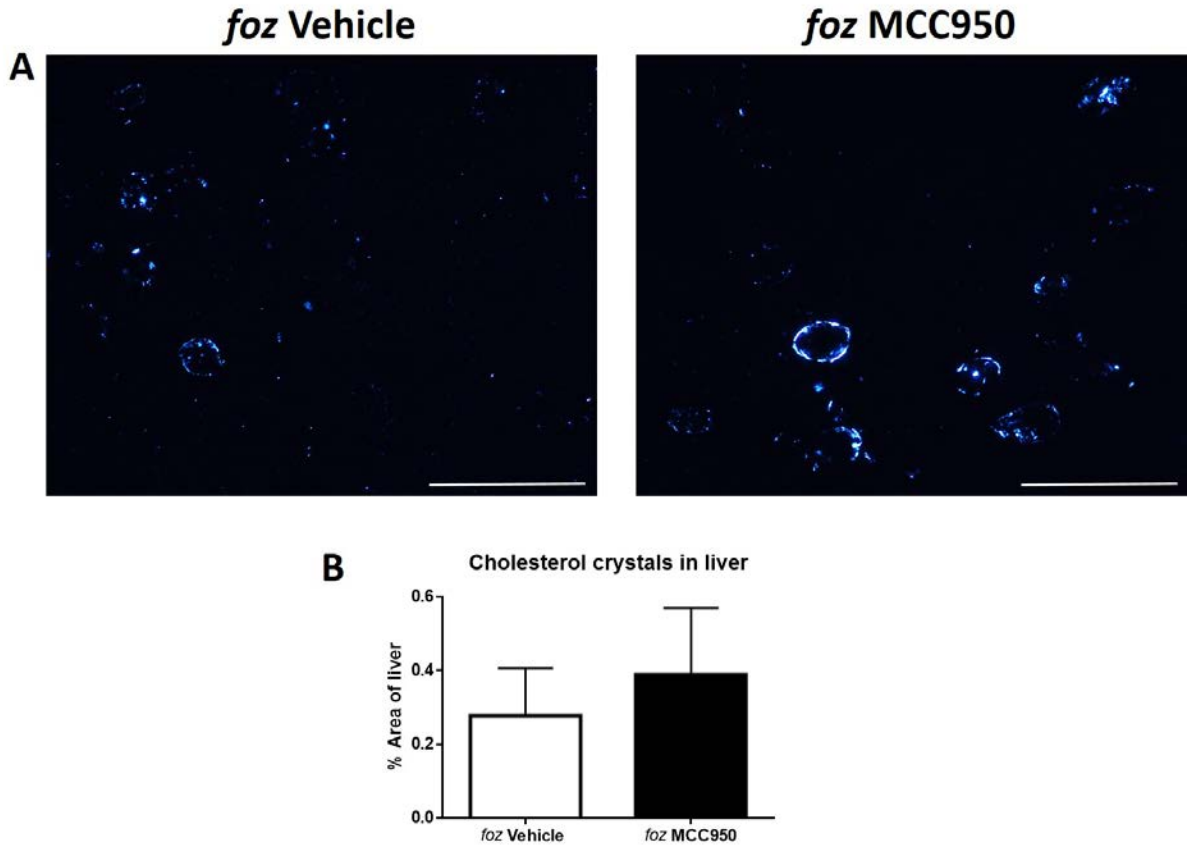

Supplementary Fig. 2. (A) Representative examples of cholesterol crystals observed by polarized light microscopy in liver sections from *foz/foz* mice at 24 weeks. Sections are from a *foz/foz* mouse treated with MCC950, and one treated with vehicle are shown (detailed methodology[1,2]). (B) Calculated area of liver sections occupied by cholesterol crystals in *foz/foz* mice administered with MCC950 or saline, and wildtype (*Wt*) mice (irrespective of treatment). Same animals as in Figs. 2-4 and 6, n=11 animals/group

.

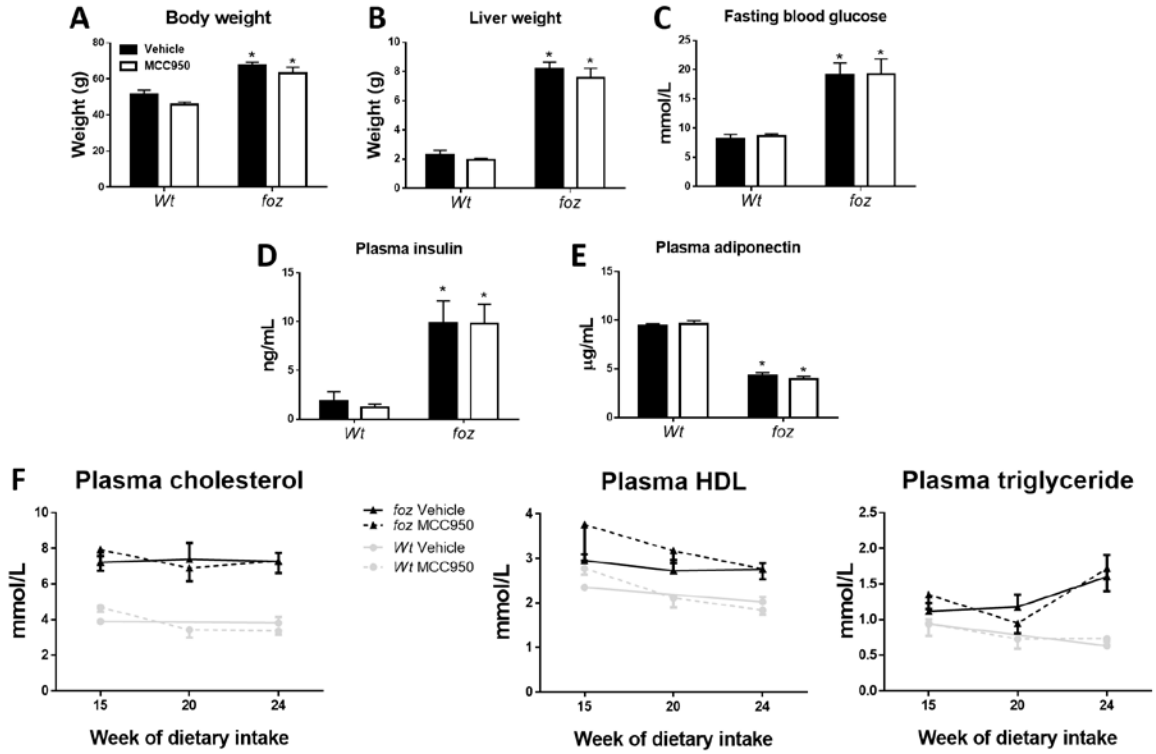

Supplementary Figure 3. (A) Body weight, (B) liver weight, (C) fasting blood glucose and (D) plasma insulin, (E) plasma adiponectin, (F) and plasma lipids (total cholesterol, high density lipoprotein cholesterol, triglycerides) in wildtype (*Wt*) and *foz/foz* mice fed atherogenic diet and gavaged from 16 weeks with MCC950 or vehicle (saline). Same animals as in Figs. 2-4 and 6. **P*<0.05 or less *versus Wt*. $^{\#}$*P*<0.05 MCC950 *versus* vehicle, by one-way ANOVA, n=11-13 animals/group.

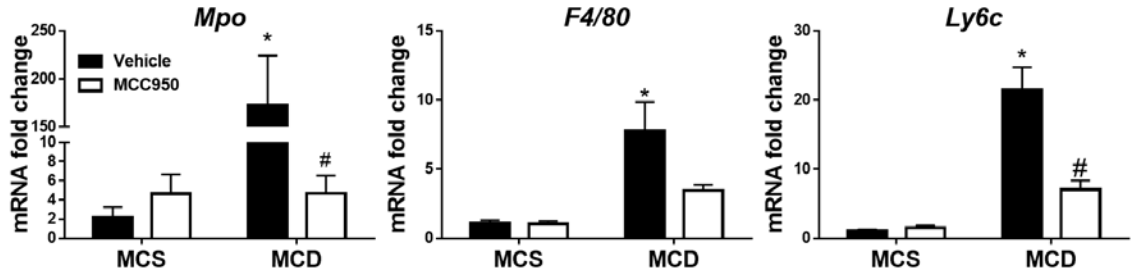

Supplementary Fig. 4. Hepatic mRNA levels for *Mpo* (neutrophils), *F4/80* (total macrophages) and *Ly6c* (inflammatory macrophages) in mice fed methionine and choline deficient (MCD) or control (methionine and choline supplemented, MCS) diets, and administered vehicle (saline) or MCC950 by gavage (same animals as Fig. 5). Data mean ± SEM, **P*<0.05 MCS *versus* MCD, #*P*<0.05 Vehicle *versus* MCC950 by ANOVA, n=8 animals/group.

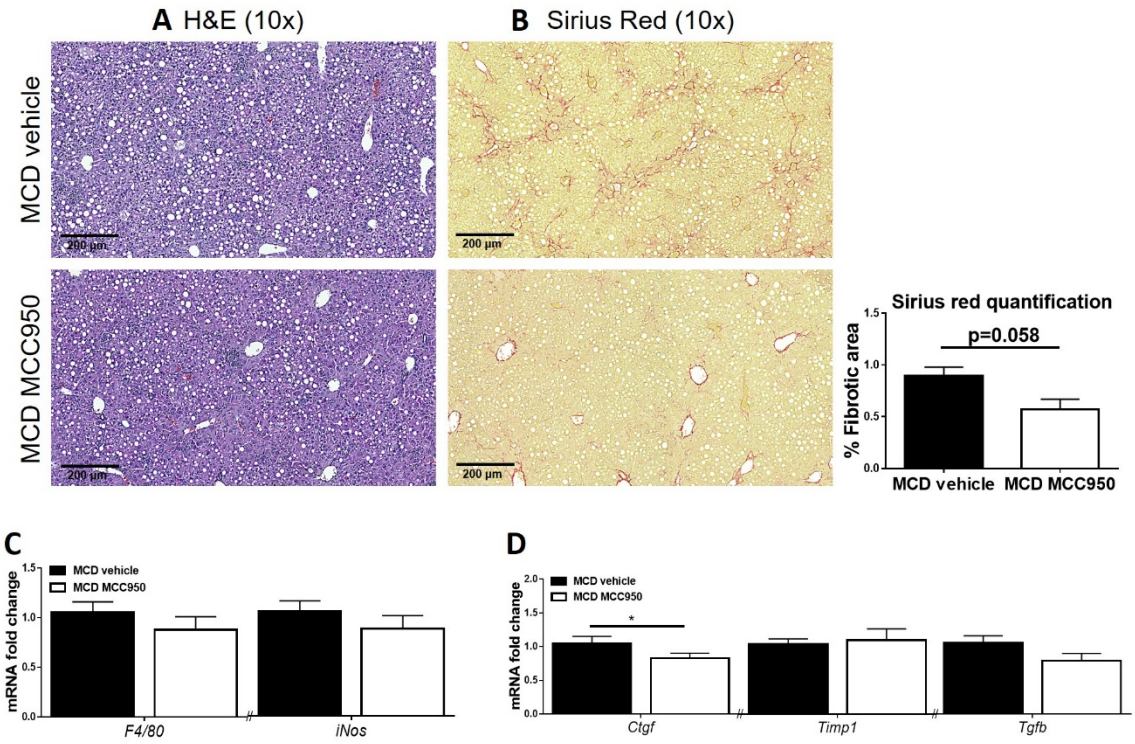

Supplementary Fig. 5. (A) Representative images of H&E and (B) Sirius red-stained liver sections, (C) hepatic mRNA levels for *Mpo* (neutrophils), *F4/80* (total macrophages) and (D) fibrosis markers (*Ctgf, Timp1* and *Tgf-*□in mice fed methionine and choline deficient (MCD) or control (methionine and choline supplemented, MCS) diets, and administered vehicle (saline) or MCC950 (20 mg/kg) by gavage for 2 weeks. Data are mean ± SEM, **P*<0.05 MCD *versus* MCS by ANOVA. n=5 animals/group.

Supplementary references

[1] Ioannou GN, Haigh WG, Thorning D, Savard C. Hepatic cholesterol crystals and crown-like structures distinguish nash from simple steatosis. J Lipid Res 2013;54:1326-1334.

[2] Ioannou GN, Van Rooyen DM, Savard C, Haigh WG, Yeh MM, Teoh NC, et al. Cholesterol-lowering drugs cause dissolution of cholesterol crystals and disperse kupffer cell crown-like structures during resolution of nash. J Lipid Res 2015;56:277-285.